

See discussions, stats, and author profiles for this publication at: <https://www.researchgate.net/publication/231730197>

# Highly Efficient Nickel–Based Heterogeneous Catalytic System with Nanosized Structural Organization for Selective Se–H Bond Addition to Terminal and Internal Alkynes

ARTICLE *in* ORGANOMETALLICS · JANUARY 2007

Impact Factor: 4.13 · DOI: 10.1021/om061033b

---

CITATIONS

47

---

READS

34

3 AUTHORS, INCLUDING:



[Valentine P. Ananikov](#)

Russian Academy of Sciences

141 PUBLICATIONS 2,841 CITATIONS

SEE PROFILE



[Nikolay V Orlov](#)

Emory University

15 PUBLICATIONS 371 CITATIONS

SEE PROFILE

# Highly Efficient Nickel-Based Heterogeneous Catalytic System with Nanosized Structural Organization for Selective Se–H Bond Addition to Terminal and Internal Alkynes

Valentine P. Ananikov,<sup>\*,†</sup> Nikolay V. Orlov,<sup>†</sup> and Irina P. Beletskaya<sup>\*,‡</sup>

Zelinsky Institute of Organic Chemistry, Russian Academy of Sciences, Leninsky Prospect 47, Moscow, 119991, Russian Federation, and Chemistry Department, Lomonosov Moscow State University, Vorob'evy gory, Moscow, 119899, Russian Federation

Received November 9, 2006

A simple heterogeneous Ni-based catalytic methodology was developed for regioselective hydroselenation of terminal alkynes and stereoselective hydroselenation of internal alkynes. The developed heterogeneous catalytic system is superior to the known homogeneous and heterogeneous catalysts for the Se–H bond addition to the triple bond of alkynes. The catalytic transformation was performed under mild conditions, thus avoiding byproducts formation. The mechanistic study revealed that the yield of the addition products depends on the catalyst particle size and rapidly increases upon decreasing particle size into the nanosized region. The present study describes a simple and efficient procedure for the formation of a self-organized nanosized catalytic system starting from an easily available precursor, Ni(acac)<sub>2</sub>, without any special treatment.

## 1. Introduction

Catalysis is one of the central fields of modern science and technology. The majority of modern industrial processes are based on heterogeneous catalysts.<sup>1</sup> Typically a heterogeneous catalyst consists of small reactive particles dispersed on a high surface area solid support. Easy separation of the solid phase ensures an important advantage of a heterogeneous catalysis: catalyst recycling. The main disadvantages of heterogeneous catalysis are insufficient selectivity, the necessity to find and maintain the optimal ratio of large surface area and high porosity, and catalyst leaching.<sup>1</sup> Of course, an important problem of heterogeneous catalysis concerns the great difficulty in studying and understanding the reaction mechanisms.<sup>2</sup>

Under homogeneous conditions all catalyst sites are accessible, and the activity and selectivity of the catalyst can be tuned by choosing appropriate ligands, solvents, and substituents.<sup>3</sup> Not surprisingly, homogeneous catalysts are widely employed in organic synthesis and have been successfully used for the preparation of natural products, biologically active compounds, drugs, and important organic building blocks.<sup>4</sup> In recent years the impact of homogeneous catalysis is increasing in industry as well,<sup>5</sup> which is further facilitated by implementing the principles of Green Chemistry.<sup>6</sup> Homogeneous catalysis does not suffer from several drawbacks of heterogeneous catalysis,

such as investigation of reaction mechanism, multiphase processes, and surface studies. However, the challenging problem of homogeneous catalysis, which limits its practical application, is catalyst separation and recycling.<sup>5</sup>

In addition to classic homogeneous and heterogeneous catalysis, the field of nanocatalysis has undergone tremendous growth during the past decade.<sup>7</sup> Using nanoparticles as catalysts made it possible to achieve important goals, such as improved activity and selectivity, low metal loading, and high surface to volume ratio, while still maintaining the advantage of easy separation and recycling.<sup>7</sup> Preparation of nanoparticles often requires specially designed procedures. An important issue to be considered is stabilization of nanoparticles toward aggrega-

\* Corresponding authors. E-mail: val@ioc.ac.ru. Fax: +007 (495) 1355328. E-mail: beletskaya@org.chem.msu.ru. Fax: +007 (495) 9393618.

<sup>†</sup> Zelinsky Institute of Organic Chemistry.

<sup>‡</sup> Lomonosov Moscow State University.

(1) (a) *Handbook of Heterogeneous Catalysis*; Ertl, G., Knoezinger, H., Weitkamp, J., Eds.; Wiley-VCH: Weinheim, Germany, 1997. (b) *Catalysis from A to Z*; Cornils, B., Herrmann, W. A., Schlögl, R., Wong, C.-H., Eds.; Wiley-VCH: Weinheim, Germany, 2000.

(2) Schlögl, R. *Angew. Chem., Int. Ed.* **1993**, 32, 381.

(3) (a) *Applied Homogeneous Catalysis with Organometallic Compounds*; Cornils, B., Herrmann, W. A., Eds.; Wiley-VCH: Weinheim, 2002. (b) *Handbook of Organopalladium Chemistry for Organic Synthesis*; Negishi, E., de Meijere, A., Eds.; John Wiley & Sons, New York, 2002. (c) *Transition Metal Catalyzed Reactions*; Murahashi, S.-I., Davies, S. G., Eds.; Blackwell Science: Oxford, 1999. (d) *Metal-Catalyzed Cross-Coupling Reactions*; Diederich, F., Stang, P. J., Eds.; Wiley-VCH: Weinheim, 1998.

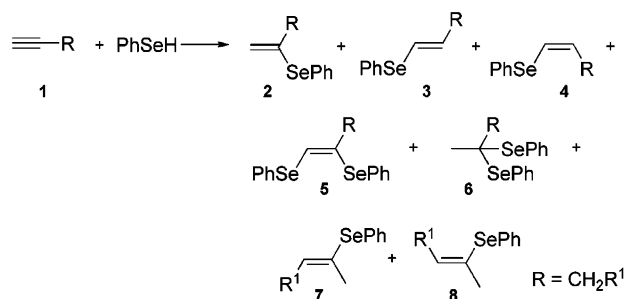
(4) Selected representative reviews: (a) Nicolaou, K. C.; Bulger, P. G.; Sarlah, D. *Angew. Chem., Int. Ed.* **2005**, 44, 4490. (b) Furstner, A. *Angew. Chem., Int. Ed.* **2000**, 39, 3012. (c) Siemsen, P.; Livingston, R. C.; Diederich, F. *Angew. Chem., Int. Ed.* **2000**, 39, 2632. (d) Beletskaya, I. P.; Cheprakov, A. V. *Chem. Rev.* **2000**, 100, 3009. (e) Suzuki, A. *J. Organomet. Chem.* **1999**, 576, 147. (f) Grubbs, R. H.; Chang, S. *Tetrahedron* **1998**, 54, 4413. (g) Miyaura, N.; Suzuki, A. *Chem. Rev.* **1995**, 95, 2457. (h) Hiyama, T.; Hatanaka, Y. *Pure Appl. Chem.* **1994**, 66, 1471. (i) Sonogashira, K. *Comp. Org. Synth.* **1991**, 3, 521. (j) Sonogashira, K. *Comp. Org. Synth.* **1991**, 3, 551. (k) Stille, J. K. *Angew. Chem., Int. Ed.* **1986**, 25, 508. (l) Negishi, E. *Acc. Chem. Res.* **1982**, 15, 340. (m) Farina, V.; Krishnamurthy, V.; Scott, W. J. *The Stille Reaction*. In *Organic Reactions*; John Wiley & Sons Inc.: New York, 1997; Vol. 50. (n) *Handbook of Metathesis*; Grubbs, R. H., Ed.; Wiley-VCH: Weinheim, 2003; Vols. 1–3.

(5) (a) Cornils, B.; Herrmann, W. A. *J. Catal.* **2003**, 216, 23–31. (b) Cole-Hamilton, D. J. *Science* **2003**, 299, 1702.

(6) (a) Trost, B. M. *Science* **1991**, 254, 1471. (b) Sheldon, R. A. *Chem. Ind.* **1992**, 903. (c) *Green Chemistry: Theory and Practice*; Anastas, P. T., Warner, J. C., Eds.; Oxford University Press: Oxford, 2000.

(7) (a) Astruc, D.; Lu, F.; Aranzas, R. *Angew. Chem., Int. Ed.* **2005**, 44, 7852. (b) Burda, C.; Chen, X.; Narayanan, R.; El-Sayed, M. A. *Chem. Rev.* **2005**, 105, 1025. (c) Grunes, J.; Zhu, J.; Somorjai, G. A. *Chem. Commun.* **2003**, 2257. (d) Bell, A. T. *Science* **2003**, 299, 1688. (e) Johnson, B. F. G. *Top. Catal.* **2003**, 24, 147. (f) Moreno-Manas, M.; Pleixats, R. *Acc. Chem. Res.* **2003**, 36, 638. (g) Buchachenko, A. L. *Russ. Chem. Rev.* **2003**, 72, 375. (h) Roucoux, A.; Schulz, J.; Patin, H. *Chem. Rev.* **2002**, 102, 3757. (i) Moiseev, I. I.; Vargaftik, M. N. *Russ. J. Gen. Chem.* **2002**, 72, 512. (j) El-Sayed, M. A. *Acc. Chem. Res.* **2001**, 34, 257. (k) Crooks, R. M.; Zhao, M.; Sun, L.; Chechik, V.; Yeung, L. K. *Acc. Chem. Res.* **2001**, 34, 181. (l) Bukhtiyarov, V. I.; Slin'ko, M. G. *Russ. Chem. Rev.* **2001**, 70, 147.

Scheme 1



tion.<sup>8</sup> A specific feature of nanoparticles is the strong dependence of activity and selectivity on the size, shape, and surface structure. For example, metal atoms located in corners and edges can be most reactive (due to free valence), while simultaneously they are likely to tear off from the particle (due to weaker bonding) or undergo a morphology change toward a more stable shape.<sup>9</sup> Losing metal atoms from the corners and edges makes the whole nanoparticle unstable and may cause quick degradation. Rapid development of electron microscopy provided a convenient tool for studying these phenomena in detail.<sup>10</sup>

In the present article we describe a new approach for designing a catalytic system with nanosized structural organization. The performance of the catalytic reaction was investigated on the model reaction of Se–H bond addition to alkynes (Scheme 1). Synthetic application of this reaction has been extensively studied in recent years, since the addition process proceeds in an atom-efficient manner without waste.<sup>11,12</sup> Depending on the reaction conditions, several products, 2–8, might be obtained (Scheme 1). The desired Markovnikov-type product 2 can be synthesized only in a transition metal-catalyzed reaction, while the anti-Markovnikov products 3 and 4 are usually formed as a result of noncatalytic Se–H bond addition to alkynes.<sup>13</sup> Therefore, the noncatalytic side-reaction leading to 3 and 4 should be suppressed under catalytic conditions. Both homogeneous<sup>14</sup> and heterogeneous<sup>15</sup> catalytic systems were developed to carry out this reaction. Homogeneous catalytic reaction was carried out using phosphine complexes of palladium. Unfortunately, in addition to the desired product 2 (20–49%), a considerable amount of another byproduct, 5 (25–40%), was also formed in this reaction.<sup>14</sup> Another homogeneous

catalytic system utilizing phosphine complexes of platinum led to 51–60% of 2. It was not possible to further increase the yield of product 2 in this system due to conversion of PhSeH to  $\text{Ph}_2\text{Se}_2$  (20–25%).<sup>14</sup> The heterogeneous catalytic system based on a Pd catalyst avoided formation of 5, but led to a mixture of 2, 6, 7, and 8.<sup>15b</sup> Compounds 7 and 8 were formed as a result of double-bond isomerization of product 2. The contribution of the isomerization reaction rapidly increases at elevated temperature.<sup>16</sup> An excellent methodology developed recently by A. Ogawa et al. has utilized  $\text{Pd}(\text{OAc})_2$  in pyridine under harsh reaction conditions (100 °C, 15 h).<sup>17</sup>

The catalytic systems developed so far operate at high temperature (80–100 °C) and require long reaction time (13–20 h). Obviously, under such conditions it is rather difficult to suppress the side-reactions and avoid byproducts formation. Another problem, which limits synthetic application of the known catalytic systems, is the increasing cost of Pd- and Pt-based catalysts. Recently, it was shown that nickel species are a cost-efficient replacement for traditional palladium catalysts in hydrothiolation of terminal alkynes.<sup>12a,18</sup> It is important to note that all catalytic systems discussed above describe Se–H bond addition to terminal alkynes, while the similar reaction involving internal alkynes has not been reported so far. In addition to regioselectivity, which is of primary importance for the addition reaction to terminal alkynes, the same process involving internal alkynes should be stereoselective as well. Therefore, the catalyst of choice should accomplish both regio- and stereoselectivity as well as high activity, since internal alkynes are noticeably less reactive. Obviously, a general synthetic method is required to perform selective Se–H bond addition to terminal and internal alkynes without byproducts formation and isomerization side-reactions.

In the present study we developed a new Ni-based catalytic system for stereo- and regioselective Se–H bond addition to terminal and internal alkynes. The reaction was performed under unusually mild conditions, therefore avoiding byproducts formation. The active form of the catalyst is generated in situ from easily available nickel compounds. We have found that optimal size and shape of the catalyst particles can be maintained by selecting different strategies at the metal compound activation stage. An electron microscopy study has suggested that catalyst organization on a nanosize scale is a key factor for achieving high catalytic activity and selectivity.

## 2. Results and Discussion

The performance of various catalytic systems was studied using model reaction of PhSeH addition to 2-methyl-3-butyne-

(8) (a) *Nanoparticles and Nanostructured Films. Preparation, Characterization and Applications*; Fendler, J. H., Ed.; Wiley-VCH: Weinheim, 1998. (b) *Nanoparticles: from Theory to Application*; Schmid, G., Ed.; Wiley-VCH: Weinheim, 2004.

(9) (a) Narayanan, R.; El-Sayed, M. A. *Nano Lett.* **2004**, *4*, 1343. (b) Narayanan, R.; El-Sayed, M. A. *J. Am. Chem. Soc.* **2004**, *126*, 7194. (c) Narayanan, R.; El-Sayed, M. A. *J. Phys. Chem. B* **2004**, *108*, 5726. (d) Li, Y.; El-Sayed, M. A. *J. Phys. Chem. B* **2001**, *105*, 8938.

(10) (a) Datye, A. K. *J. Catal.* **2003**, *216*, 144. (b) Topsoe, H. *J. Catal.* **2003**, *216*, 155. (c) Hansen, T. W.; Wagner, J. B.; Hansen, P. L.; Dahl, S.; Topsoe, H.; Jacobsen, C. J. H. *Science* **2001**, *294*, 1508. (d) Sachs, C.; Hildebrand, M.; Volkening, S.; Winterlin, J.; Ertl, G. *Science* **2001**, *293*, 1635.

(11) (a) Alonso, F.; Beletskaya, I. P.; Yus, M. *Chem. Rev.* **2004**, *104*, 3079. (b) Beller, M.; Seayad, J.; Tillack, A.; Jiao, H. *Angew. Chem., Int. Ed.* **2004**, *43*, 3368. (c) Kondo, T.; Mitsudo, T. *Chem. Rev.* **2000**, *100*, 3205.

(12) For a similar reaction of S–H bond addition to alkynes see: (a) Ananikov, V. P.; Malyshev, D. A.; Beletskaya, I. P.; Aleksandrov, G. G.; Eremenko, I. L. *Adv. Synth. Catal.* **2005**, *347*, 1993. (b) Malyshev, D. A.; Scott, N. M.; Marion, N.; Stevens, E. D.; Ananikov, V. P.; Beletskaya, I. P.; Nolan, S. P. *Organometallics* **2006**, *25*, 4462. (c) Han, L.-B.; Zhang, C.; Yazawa, H.; Shimada, S. *J. Am. Chem. Soc.* **2004**, *126*, 5080. (d) Ogawa, A.; Ikeda, T.; Kimura, K.; Hirao, T. *J. Am. Chem. Soc.* **1999**, *121*, 5108. (e) Backvall, J.-E.; Ericsson, A. *J. Org. Chem.* **1994**, *59*, 5850. (f) Kuniyasu, H.; Ogawa, A.; Sato, K.; Ryu, I.; Kambe, N.; Sonoda, N. *J. Am. Chem. Soc.* **1992**, *114*, 5902.

(13) Noncatalytic addition of a Se–H bond to alkynes leads to anti-Markovnikov isomers 3 and 4; see: (a) Potapov, V. A.; Amosova, S. V. *Russ. J. Org. Chem.* **1996**, *32*, 1099. (b) Ogawa, A.; Obayashi, R.; Sekiguchi, M.; Masawaki, T.; Kambe, N.; Sonoda, N. *Tetrahedron Lett.* **1992**, *33*, 1329. (c) Kataoka, T.; Yoshimatsu, M.; Shimizu, H.; Hori, M. *Tetrahedron Lett.* **1990**, *31*, 5927. (d) Comasseto, J. V.; Brandt, C. A. *Synthesis* **1987**, 146. (e) Renard, M.; Hevesi, L. *Tetrahedron* **1985**, *41*, 5939. (f) Tsoi, L. A.; Patsaev, A. K.; Ushanov, V. Zh.; Vyaznikovtsev, L. V. *J. Org. Chem. USSR (Engl. Transl.)* **1984**, 1897. (g) Comasseto, J. V. *J. Organomet. Chem.* **1983**, *253*, 131. (h) Kataev, E. G.; Petrov, V. N. *J. Gen. Chem. USSR (Engl. Transl.)* **1962**, *32*, 3626.

(14) Ananikov, V. P.; Malyshev, D. A.; Beletskaya, I. P.; Aleksandrov, G. G.; Eremenko, I. L., *J. Organomet. Chem.* **2003**, *679*, 162.

(15) (a) Ogawa, A. *J. Organomet. Chem.* **2000**, *611*, 463. (b) Kuniyasu, H.; Ogawa, A.; Sato, K.-I.; Ryu, I.; Sonoda, N. *Tetrahedron Lett.* **1992**, *33*, 5525.

(16) The isomerization reaction may proceed under transition metal-catalyzed, radical, or photochemical conditions (see refs 12, 14, 15).

(17) Kamiya, I.; Nishinaka, E.; Ogawa, A. *J. Org. Chem.* **2005**, *70*, 696.

(18) Ananikov V. P.; Orlov N. V.; Beletskaya I. P. *Organometallics* **2006**, *25*, 970.

**Table 1.** Various Metal Complexes as Catalyst Precursors for the PhSeH Addition to **1a**<sup>a</sup>

entry	catalyst precursor	yield of <b>2a</b> , <sup>b</sup> %	<b>2a:3a</b> ratio <sup>b</sup>
1	Pd(PPh <sub>3</sub> ) <sub>4</sub>	2 <sup>d</sup>	
2	Pd(OAc) <sub>2</sub>	17	99:1
3	NiCl <sub>2</sub>	6	75:25
4	Ni(OAc) <sub>2</sub>	21	91:9
5	NiCl <sub>2</sub> ·Et <sub>3</sub> N <sup>c</sup>	38	94:6
6	Ni(OAc) <sub>2</sub> ·Et <sub>3</sub> N <sup>c</sup>	59	92:8
7	Ni(acac) <sub>2</sub>	74	93:7
8	Ni(acac) <sub>2</sub> ·Et <sub>3</sub> N <sup>c</sup>	56	93:7

<sup>a</sup> Using 1.2 mmol of PhSeH, 1 mmol of alkyne, and 2 mol % of the catalyst under solvent-free conditions at 25 °C for 10 min. <sup>b</sup> Determined by NMR. <sup>c</sup> With 4 mol % of Et<sub>3</sub>N. <sup>d</sup> About 1% of **5a** was also formed.

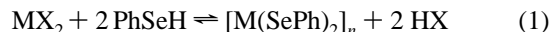
2-ol (**1a**). The absence of allylic hydrogens avoids isomerization of **2** to **7** and **8**, thus simplifying conditions for optimization of catalyst activity and selectivity.<sup>19</sup> The model reactions were carried out under solvent-free conditions at 25 °C for a short time of 10 min. The well-studied Pd catalytic system was chosen as a reference for comparison (entries 1, 2; Table 1). Homogeneous reaction with Pd(PPh<sub>3</sub>)<sub>4</sub> precursor under mild conditions gave only 2% of the PhSeH addition product (entry 1; Table 1). Using Pd(OAc)<sub>2</sub> as a catalyst precursor in heterogeneous reaction resulted in 17% of **2a** (entry 2, Table 1). NiCl<sub>2</sub> showed rather poor performance, giving 6% of **2a** and 75:25 selectivity<sup>20</sup> (entry 3, Table 1). Better results were achieved using Ni(OAc)<sub>2</sub> as a catalyst precursor: 21% of **2a** and 91:9 selectivity (entry 4, Table 1).

We have found that a catalytic amount of Et<sub>3</sub>N dramatically increases the yield and selectivity of PhSeH addition to **1a**. Utilizing 2 mol % of NiCl<sub>2</sub> and 4 mol % of Et<sub>3</sub>N led to a 6-fold increase in the yield of **2a** (38%) and improved the selectivity to 94:6 (entry 5, Table 1), compared to the same reaction without Et<sub>3</sub>N (6% of **2a**, 75:25 selectivity; see entry 3, Table 1). Significant enhancement was also observed in the case of Ni(OAc)<sub>2</sub> (cf. entries 4 and 6, Table 1). The catalytic system utilizing Ni(acac)<sub>2</sub> as a catalyst precursor made it possible to achieve a high yield of 74% and excellent selectivity (93:7) under the same conditions (entry 7, Table 1). Addition of Et<sub>3</sub>N did not further improve the performance of the catalytic system; moreover the yield decreased to 56% (entry 8, Table 1). To understand the observed large difference in catalytic activity of various metal complexes, we have performed a detailed mechanistic study.

Under homogeneous conditions (entry 1, Table 1) the active form of the catalyst is represented by dinuclear complexes *cis*- and *trans*-[Pd<sub>2</sub>(SePh)<sub>4</sub>(PPh<sub>3</sub>)<sub>2</sub>],<sup>21</sup> which catalyze both Se–H and Se–Se bond addition to alkynes, leading to **2** and **5**, respectively.<sup>22</sup> Phosphine ligands facilitate the C–Se reductive

elimination, the key stage of compound **5** formation.<sup>12a</sup> The <sup>31</sup>P NMR monitoring has confirmed the presence of the dinuclear complexes under catalytic conditions at 25 °C, in agreement with the mechanistic study performed at 80 °C.<sup>22</sup>

Under heterogeneous conditions (entries 2–4, 7; Table 1) insoluble polymeric [M(SePh)<sub>2</sub>]<sub>n</sub> species<sup>23</sup> were formed according to the following substitution reaction (M = Ni, Pd; X = Cl, OAc, acac):

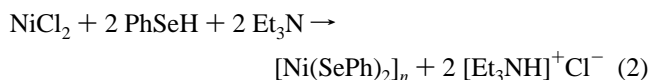


Scanning electron microscopy (SEM) study of the palladium catalyst has revealed the particles to be in micrometer size scale, 3–6 μm (entry 1, Table 2). A typical SEM image is shown in Figure 1A. Catalyst particles possess different shapes with non-uniform structure. Similar morphology was observed for the catalyst formed from NiCl<sub>2</sub> and Ni(OAc)<sub>2</sub> precursors (entries 2, 3, Table 2; Figures 1B and 1C). In the later case somewhat smaller particles were observed with more “crumbly” structure. Smaller particle size results in higher surface-to-volume ratio, while “crumbly” structure ensures more accessible sites. According to elemental analysis complete ligand substitution (eq 1) takes place for Pd(OAc)<sub>2</sub> and Ni(OAc)<sub>2</sub> precursors (entries 1, 3; Table 2). For NiCl<sub>2</sub> only a small amount of chloride ligands were replaced by SePh (entry 2, Table 2). Most likely, these are the reasons for the higher catalytic activity in the reaction involving Ni(OAc)<sub>2</sub> compared to NiCl<sub>2</sub> (cf. entries 3, 4, Table 1).

Very surprising results were achieved upon investigation of the NiCl<sub>2</sub>/Et<sub>3</sub>N catalytic system. As shown on a low-magnification SEM image of the catalyst (Figure 2A), it is a complex three-dimensional network consisting of nanosized crystals with supported particles. Washing the catalyst with water or methanol resulted in the disappearance of network structure (Figure 2B). The remaining insoluble part was identified as [Ni(SePh)<sub>2</sub>]<sub>n</sub> according to elemental analysis, while an NMR study of the methanol solution confirmed the presence of [Et<sub>3</sub>NH]<sup>+</sup>Cl<sup>−</sup>. Therefore, the catalyst consists of [Ni(SePh)<sub>2</sub>]<sub>n</sub> particles adsorbed on the [Et<sub>3</sub>NH]<sup>+</sup>Cl<sup>−</sup> crystals. Analysis of the SEM images with higher magnification (Figures 2C and 2D) gave the following size of the [Et<sub>3</sub>NH]<sup>+</sup>Cl<sup>−</sup> crystals: 0.2–3 μm width, 10–70 μm length, and 50–250 nm thickness. The size of the nickel-containing particles was 0.3–1.5 μm (entry 4, Table 2).

A high degree of networking prevents aggregation of the nickel particles, maintaining a high surface-to-volume ratio of the catalyst during the addition reaction. Interconnected and periodically spaced features of the network with certain 3D void spaces made the catalyst sites more accessible by the substrate molecules. As a result, much better yield and selectivity were observed in the presence of Et<sub>3</sub>N (cf. entries 3 and 5; Table 1).

It should be noted that both catalyst and support were formed in a single step upon reaction of the precursor compound with the substrate in the presence of Et<sub>3</sub>N:



(19) The possibility of the **2** → **7** + **8** isomerization will be elaborated later on the other alkynes.

(20) The selectivity of the addition reactions is reflected by the ratio of Markovnikov and anti-Markovnikov products (**2**)/(**3**+**4**).

(21) (a) Hannu-Kuure, M. S.; Wagner, A.; Bajorek, T.; Oilunkaniemi, R.; Laitinen, R. S.; Ahlgren, M. *Main Group Chem.* **2005**, *4*, 49. (b) Hannu-Kuure, M. S.; Paldan, K.; Oilunkaniemi, R.; Laitinen, R. S.; Ahlgren, M. *J. Organomet. Chem.* **2003**, *687*, 538. (c) Oilunkaniemi, R.; Laitinen, R. S.; Ahlgren, M. *J. Organomet. Chem.* **2001**, *623*, 168. (d) Dey, S.; Jain, V. K.; Varghese, B. *J. Organomet. Chem.* **2001**, *623*, 48. (e) Oilunkaniemi, R.; Laitinen, R. S.; Ahlgren, M. *J. Organomet. Chem.* **1999**, *587*, 200.

(22) (a) Ananikov, V. P.; Kabeshov, M. A.; Beletskaya, I. P.; Khurstalev, V. N.; Antipin, M. Yu. *Organometallics* **2005**, *24*, 1275. (b) Ananikov, V. P.; Beletskaya, I. P.; Aleksandrov, G. G.; Eremanko, I. L. *Organometallics* **2003**, *22*, 1414. (c) Ananikov, V. P.; Kabeshov, M. A.; Beletskaya, I. P.; Aleksandrov, G. G.; Eremanko, I. L. *J. Organomet. Chem.* **2003**, *687*, 451. (d) Ananikov, V. P.; Beletskaya, I. P. *Org. Biomol. Chem.* **2004**, *2*, 284.

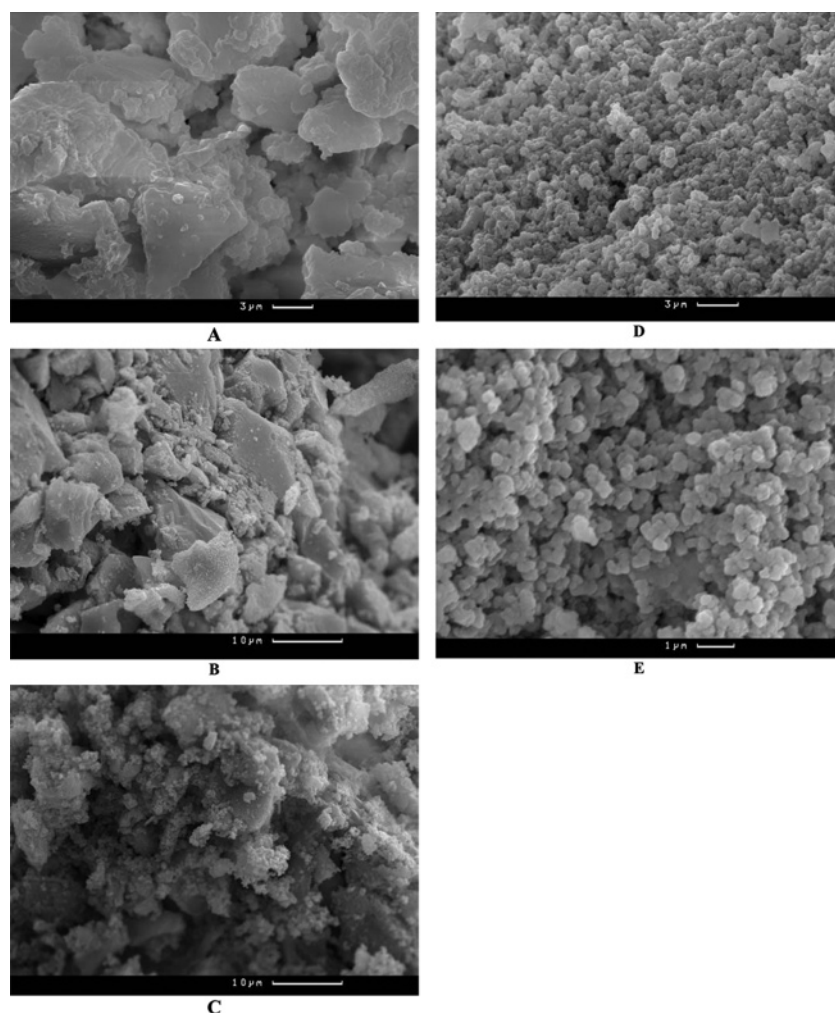
(23) For a related discussion concerning the structure and formation of polynuclear transition metal arylselenolates see refs 21 and 22.



Table 2. Scanning Electron Microscopy Study of the Catalysts

entry	catalyst precursor	procedure <sup>a</sup>	catalyst active form <sup>b</sup>	particle size <sup>c</sup>	morphology
1	Pd(OAc) <sub>2</sub>	1) alkyne <b>1a</b> ; 2) PhSeH	[Pd(SePh) <sub>2</sub> ] <sub>n</sub>	3–6 μm	nonuniform shape, amorphous structure
2	NiCl <sub>2</sub>	1) alkyne <b>1a</b> ; 2) PhSeH	Ni(SePh) <sub>2</sub> :NiCl <sub>2</sub> = 1:9	3–10 μm	nonuniform shape, amorphous structure
3	Ni(OAc) <sub>2</sub>	1) alkyne <b>1a</b> ; 2) PhSeH	[Ni(SePh) <sub>2</sub> ] <sub>n</sub>	2–5 μm	nonuniform shape, amorphous structure
4	NiCl <sub>2</sub>	1) alkyne <b>1a</b> ; 2) PhSeH; 3) Et <sub>3</sub> N	[Ni(SePh) <sub>2</sub> ] <sub>n</sub> / 2n[Et <sub>3</sub> NH] <sup>+</sup> Cl <sup>−</sup>	0.3–1.5 μm	nonuniform shape, aggregated particles supported on the [Et <sub>3</sub> NH] <sup>+</sup> Cl <sup>−</sup> crystals <sup>d</sup>
5	Ni(acac) <sub>2</sub>	1) alkyne <b>1a</b> ; 2) PhSeH	[Ni(SePh) <sub>2</sub> ] <sub>n</sub>	200–400 nm	uniform shape, nanostructured building units
6	Ni(acac) <sub>2</sub>	1) PhSeH; 2) alkyne <b>1a</b>	[Ni(SePh) <sub>2</sub> ] <sub>n</sub>	2–8 μm	nonuniform shape, amorphous structure, wide distribution of particles sizes
7	Ni(acac) <sub>2</sub>	recycled	[Ni(SePh) <sub>2</sub> ] <sub>n</sub>	0.2–1.0 μm	nonuniform shape, nanostructured building units and aggregated particles

<sup>a</sup> See Experimental Section for other details. <sup>b</sup> According to elemental analysis data (see Experimental Section). <sup>c</sup> The range of particle sizes estimated by SEM. <sup>d</sup> See text for the [Et<sub>3</sub>NH]<sup>+</sup>Cl<sup>−</sup> crystal size.



**Figure 1.** SEM images of catalyst particles prepared from different precursors: Pd(OAc)<sub>2</sub> (A) (4000×); NiCl<sub>2</sub> (B) (2000×); Ni(OAc)<sub>2</sub> (C) (2000×); Ni(acac)<sub>2</sub> (D) (4000×); Ni(acac)<sub>2</sub> (E) (10000×).

Therefore, Et<sub>3</sub>N plays a dual role in the studied system. On one hand it shifts the equilibrium and ensures complete chloride ligand substitution by SePh (cf. eq 1), on the other hand it leads to formation of the [Et<sub>3</sub>NH]<sup>+</sup>Cl<sup>−</sup> catalyst support (see eq 2).

The smallest catalyst particles were prepared utilizing Ni(acac)<sub>2</sub> as catalyst precursor. In this case approximately spherically shaped<sup>24</sup> uniform particles (Figures 1D, 1E) of 200–400 nm size were formed (entry 5, Table 2). The order of reagent

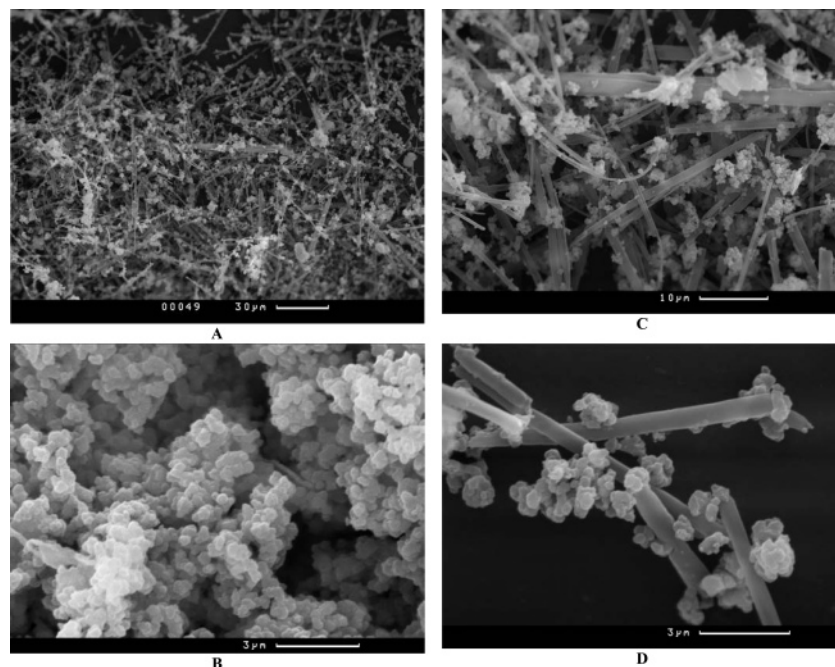


**Figure 2.** SEM images of the catalyst prepared in the  $\text{NiCl}_2/\text{Et}_3\text{N}$  system at various magnification levels: (A) 500 $\times$ , (C) 2000 $\times$ , (D) 9000 $\times$ ; (B) catalyst prepared in the  $\text{NiCl}_2/\text{Et}_3\text{N}$  system and washed with water (8000 $\times$ ).

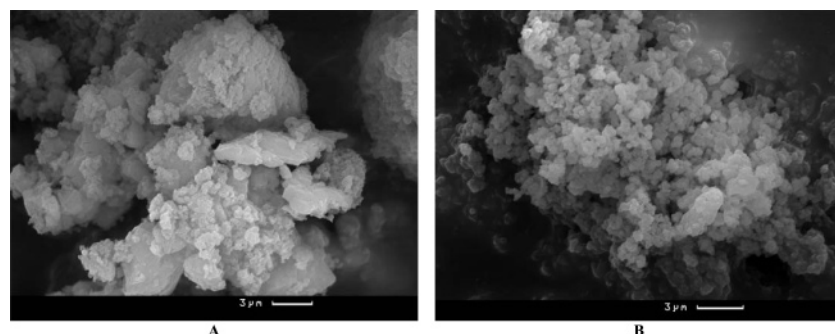


**Figure 3.** SEM images of the catalyst prepared from  $\text{Ni}(\text{acac})_2$  using reversed sequence of reagent addition (A) (4000 $\times$ ) and recycled catalyst (B) (4500 $\times$ ).

addition plays crucial role in the formation of these catalytic sites. If the catalyst precursor  $\text{Ni}(\text{acac})_2$  was mixed and stirred with alkyne followed by addition of  $\text{PhSeH}$ , an active catalyst with nanosized structural organization was formed (entry 5, Table 2). The reversed order of reagent addition, i.e., stirring  $\text{Ni}(\text{acac})_2$  with  $\text{PhSeH}$ , followed by addition of the alkyne, leads to a less active catalyst. In this case about 45% of **2a** was formed after 10 min at 25 °C (cf. 74%, entry 7, Table 1). Comparing SEM images of both catalysts (Figures 1E and 3A, respectively) clearly indicates that the reversed order of reagent addition gave larger particles sizes without nanosized structural organization (entry 6, Table 2). Examination of both catalyst preparation procedures showed that  $\text{Ni}(\text{acac})_2$  is partially soluble in alkynes.<sup>25</sup> Precipitation of  $[\text{Ni}(\text{SePh})_2]_n$  from the suspension of  $\text{Ni}(\text{acac})_2$  in alkyne provides the best conditions for nanosized building unit formation.  $\text{NiCl}_2$  and  $\text{Ni}(\text{OAc})_2$  are less soluble in alkynes and, consequently, gave another catalyst structure (cf. entries 2, 3, and 5; Table 2) with lower catalytic activity in the reaction of interest (cf. entries 3, 4, and 7; Table 1). Comparing SEM images of Pd and Ni catalysts (Figures 1A and 1D, respectively)

at the same magnification (4000 $\times$ ) clearly outlines principal differences between these systems.

The study of the catalyst structure and morphology clearly showed that immobilization of the catalyst particles into a solid support increases catalyst activity and selectivity. However, even better results can be obtained without any support in the case of smaller spherically shaped catalyst particles. It is worthy of note that spherically shaped particles have the most stable surface toward reconstruction during the course of the reaction.

As shown in Table 2, all the catalysts have the same chemical composition  $[\text{M}(\text{SePh})_2]_n$ ; however the catalytic activity dramatically differs (Table 1). In the studied catalytic system the linear dependence of the product yields versus the size of catalyst particles has been observed for the particle sizes > 1  $\mu\text{m}$  (Figure 4). Interestingly, both Ni and Pd complexes lie on the same curve, indicating that size effect is more important compared to the metal effect. Decreasing particle size into the nanoregion greatly increases catalyst activity, in an exponential manner, as shown for the catalyst generated from  $\text{Ni}(\text{acac})_2$  (Figure 4).

The scope of the developed catalytic system was investigated for a variety of terminal alkynes with different functional groups (Table 3). Most of the reactions were carried out at 20–40 °C for 20–90 min (entries 1–5, Table 3). The products **2b** and

(24) The particles obtained in other cases are far from round shaped (see Figure 1A–C).

(25) The solubility depends on the alkyne; for example  $\text{Ni}(\text{acac})_2$  is completely soluble in phenylacetylene (**1h**), while in 2-methyl-3-butyne-2-ol (**1a**) the suspension was formed.

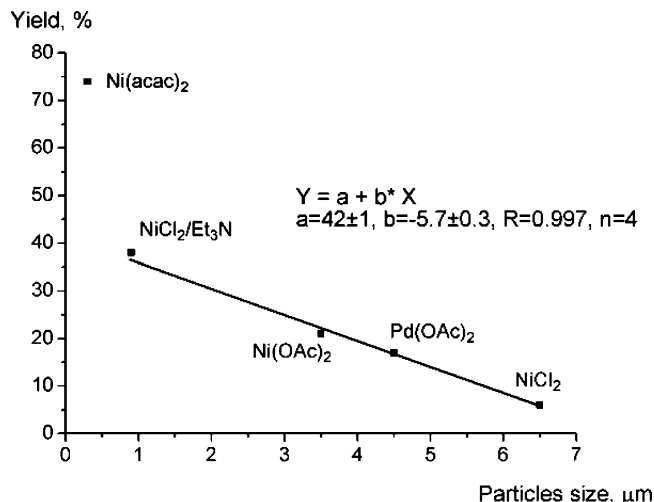


**Figure 4.** Plot of the product **2a** yields measured after 10 min of reaction time vs average sizes of the  $[\text{Ni}(\text{SePh})_2]_n$  catalyst particles (the yields are given in Table 1; particle sizes in Table 2). The catalyst precursor is shown for each point; the linear regression analysis has been performed for all points excluding  $\text{Ni}(\text{acac})_2$ .

**2c**, with allylic hydrogens, did not undergo an isomerization reaction to **7** and **8** during the catalytic reaction (entries 2, 3; Table 3). Performing the reaction with sterically hindered alkyne **1f** required higher temperature and longer heating (60 °C, 4 h) for completion of the PhSeH addition (entry 6, Table 3). Alkyne **1g**, bearing OAc group, was also less active in the addition reaction (cf. entries 1 and 7, Table 3), resulting in excellent yield (99%) and excellent selectivity (97:3) after 3.5 h at 40 °C.

The reaction with activated alkynes deserves special note. To reduce the contribution of the noncatalytic processes, the reaction with phenylacetylene (**1h**) was carried out at −5 °C. The Markovnikov-type compound **2h** was the major product of the addition reaction (entry 8, Table 3). Even in a very challenging case of a highly activated alkyne—methylpropiolate (**1i**)—some amount of Markovnikov product was obtained (entry 9, Table 3). The structures of the products **2a–2i** were established using 2D NMR experiments, COSY, NOESY, HMQC, and HMBC.

The products **2a–2g** were purified with flash chromatography for removing trace amounts of **3a–3g**. GC-MS and NMR examination of late chromatography fractions revealed the formation of small amounts (4–11%) of dienes with general formula  $\text{H}_2\text{C}=\text{CR}-\text{CH}=\text{C}(\text{SePh})\text{R}$  or  $\text{H}_2\text{C}=\text{CR}-\text{C}(\text{SePh})=\text{CHR}$ . Such dienes might be obtained as a result of condensation of two alkyne molecules with PhSeH. This interesting feature of the nickel-catalyzed reaction will be addressed in detail later and reported elsewhere.

It is interesting to consider the origin of the anti-Markovnikov species **3** obtained for nonactivated alkynes **1a–1g** in the studied catalytic system. Carrying out the reactions at the same temperature and time, but without the Ni complex, gave no evidence for the formation of **3**, while under the catalytic conditions small amounts of *E*-isomers **3** were detected (entries 1–7, Table 3).<sup>26</sup> Therefore, we have proposed that isomer **3** was formed as a result of Ni-catalyzed transformation. The major product **2** was formed via pathway A and the minor product **3** via pathway B (Scheme 2). Steric repulsion between the R group and metal center in the intermediate metal complex makes pathway B less favorable.<sup>27</sup>

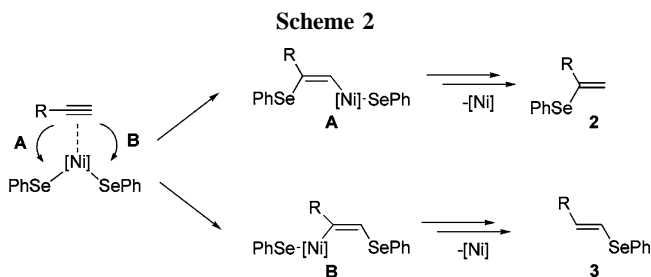
(26) The compounds **3** and **4** can be easily distinguished by <sup>1</sup>H NMR taking into account that the <sup>3</sup>J(H–H) coupling constant is 12–16 Hz for **3** and 7–11 Hz for **4**.

**Table 3.** Ni-Catalyzed PhSeH Addition to Terminal Alkynes<sup>a</sup>

Entry	Alkyne	Product	Conditions	Yield, % <sup>b</sup>
1			30 min, 20 °C	90 92:8:0 <sup>c</sup>
2			20 min, 20 °C	87 84:16:0 <sup>c</sup>
3			50 min, 20 °C	87 87:13:0 <sup>c</sup>
4			30 min, 40 °C	91 90:10:0 <sup>c</sup>
5			1.5 h, 20 °C	93 93:7:0 <sup>c</sup>
6			4 h, 60 °C	94 89:11:0 <sup>c</sup>
7			3.5 h, 40 °C	99 97:3:0 <sup>c</sup>
8			20 min, −5 °C	99 49:40:10 <sup>c</sup>
9			20 min, −5 °C	99 16:73:11 <sup>c</sup>

<sup>a</sup> Using 1.2 mmol of PhSeH, 1 mmol of alkyne, and 2 mol % of  $\text{Ni}(\text{acac})_2$  under solvent-free conditions (see Experimental Section for details). <sup>b</sup> The yield of addition products (**2**+**3**+**4**) determined by NMR after completion of the reaction (the isolated yields are given in the Experimental Section).

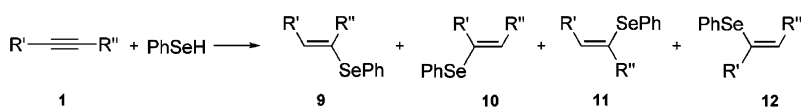
<sup>c</sup> The ratio of the **2**:**3**:**4** isomers (see Scheme 1) determined by NMR after completion of the reaction.

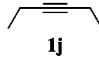
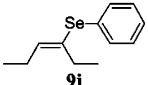
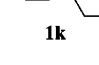
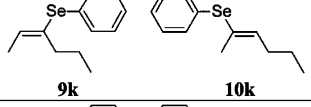
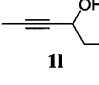
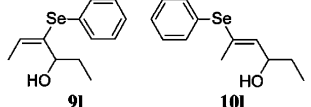
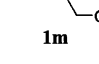
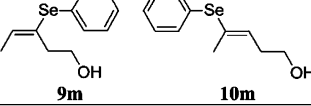
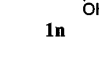
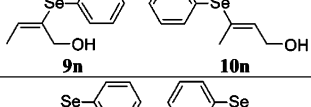
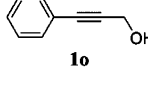
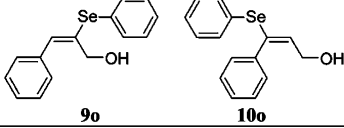
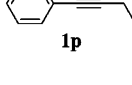
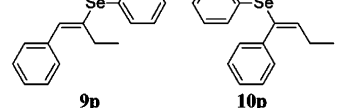


The developed catalytic system was successfully utilized for the PhSeH addition not only to terminal alkynes but to an internal  $\text{C}\equiv\text{C}$  bond as well. In the case of internal alkyne four isomers might be expected depending on the regio- and stereoselectivity of the reaction (Scheme 3). In the studied case only *syn*-addition products (**9** and **10**) were formed with high

(27) Electronic effect and coordination of oxygen atom to Ni could also make some contribution to the relative stability of the intermediate complexes.

Scheme 3

Table 4. Ni-Catalyzed PhSeH Addition to Internal Alkynes<sup>a</sup>

Entry	Alkyne	Product	Conditions	Yield, <sup>b</sup> %
1			6 h, 25°C	99
2			5 h, 25°C	93 66:34 <sup>c</sup>
3			16 h, 25°C	86 79:21 <sup>c</sup>
4			7 h, 40°C	92 60:40 <sup>c</sup>
5			3 h, 40°C	88 62:38 <sup>c</sup>
6			2 h, 40°C	99 68:32 <sup>c</sup>
7			5 h, 25°C	99 78:22 <sup>c</sup>

<sup>a</sup> Using 1.2 mmol of PhSeH, 1 mmol of alkyne, and 2 mol % of Ni(acac)<sub>2</sub> under solvent-free conditions (see Experimental Section for details). <sup>b</sup> The yield of addition products (**9**–**12**) determined by NMR after completing the reaction (the isolated yields are given in the Experimental Section). <sup>c</sup> The ratio of the **9** and **10** isomers (see Scheme 3) determined by NMR after completing the reaction.

stereoselectivity (>99:1). The formation of *anti*-addition products (**11** and **12**) was not observed. The geometry of the double bond was established by a 2D NOESY experiment, and the structures of the products were determined using 2D COSY, HMQC, and HMBC experiments. Under solvent-free conditions at 25–40 °C the reaction with 2 mol % of Ni(acac)<sub>2</sub> catalyst precursor was carried out with excellent yields of 86–99% (Table 4). Internal alkynes were less reactive than terminal ones and required a longer time of 2–16 h (Table 4).

A single product was prepared in the case of symmetric alkyne **1j** (R = R' = Et), and a mixture of isomers **9** and **10** was obtained in the reactions involving nonsymmetric alkynes (cf. entries 1 and 2–7; Table 4). The regioisomers **9** and **10** were separated with flash chromatography on silica and isolated in pure form. It is interesting to note that dienes were not detected in the case of internal alkynes (see discussion above for terminal alkynes). The absence of the side-reaction leading to dienes resulted in better yields of addition products compared to the terminal alkynes (cf. Table 4 and Table 3).

We found that the regioselectivity of the reaction does not depend in a substantial way on the presence of oxygen atoms for both alkyl-substituted (cf. **1k** with **1l** and **1m**; Table 4) and aryl-substituted (cf. **1o** and **1p**; Table 4) alkynes. This suggests that alkyne coordination to the metal complex in chelate fashion

did not govern the regioselectivity of the addition reaction in the studied catalytic system.

The plausible mechanism of the catalytic reaction is shown in Scheme 4.<sup>28</sup> The catalytic cycle involves (i) catalyst activation via acac ligand substitution by PhSeH in the presence of alkyne; (ii) coordination of alkyne on the polymeric catalyst **13** and alkyne insertion into the Ni–Se bond; and (iii) protonolysis of the Ni–C bond by PhSeH leading to regeneration of the catalyst and formation of product **2** (**9**, **10**). Stereochemistry of the products **9** and **10** clearly confirms that the addition reaction proceeds in a *syn*-manner involving alkyne insertion into the metal–selenium bond.

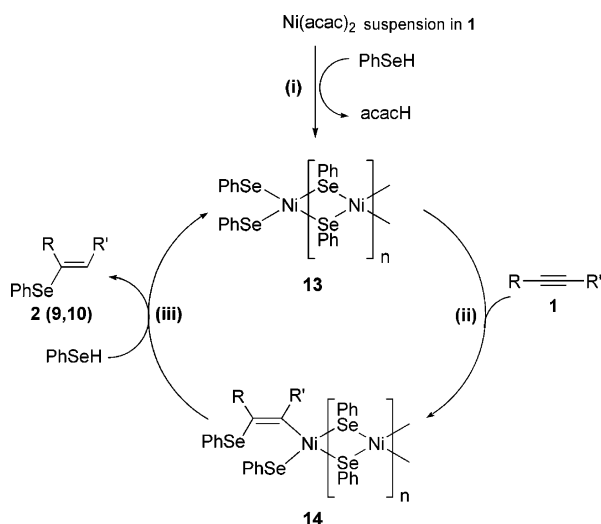
To confirm the proposed mechanism, a sequence of stoichiometric reactions was carried out (Scheme 5). The polymeric complex [Ni(SePh)<sub>2</sub>]<sub>n</sub> was prepared according to reaction of Ni(acac)<sub>2</sub> with PhSeH and was isolated (see Experimental Section for details). In the presence of 1 equiv of PhSeH compound **2a** was formed in good yield at 40 °C (80%). In the absence of PhSeH the formation of **2a** from [Ni(SePh)<sub>2</sub>]<sub>n</sub> and **1a** did not take place even after heating at 60 °C for 4 h.

Catalyst recycling in Ni-based catalytic systems is less economically important compared with Pd, Pt, and Rh ana-

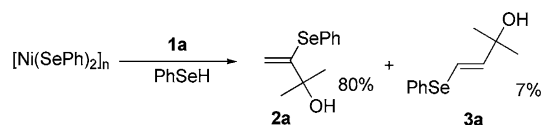
(28) The reaction pathway leading to the minor product **3** (for R' = H) was omitted for simplicity.



Scheme 4



Scheme 5

Table 5. Catalyst Recycling in the PhSeH Addition to **1a** Catalyzed by Ni Complexes

cycle	catalyst isolation <sup>a</sup>		"fresh start" <sup>b</sup>	
	yield of <b>2a</b> , <sup>c</sup> %	<b>2a</b> : <b>3a</b> ratio <sup>c</sup>	yield of <b>2a</b> , <sup>c</sup> %	<b>2a</b> : <b>3a</b> ratio <sup>c</sup>
1	90	93:7	90	93:7
2	61	93:7	76	93:7
3	41	93:7	68	93:7

<sup>a</sup> First cycle: using 1.2 mmol of PhSeH, 1 mmol of alkyne, and 2 mol % of the catalyst under solvent-free conditions at 40 °C for 10 min; other cycles: recycled catalyst in the same conditions (see Experimental Section for further details). <sup>b</sup> First cycle: using 1.2 mmol of PhSeH, 1 mmol of alkyne, and 2 mol % of the catalyst under solvent-free conditions at 40 °C for 10 min; other cycles: new portions of PhSeH and **1a** were added without catalyst isolation (see Experimental Section for further details). <sup>c</sup> Determined by NMR.

logues. Anyway we have investigated the possibility of catalyst recycling in order to understand the process of catalyst aging. Recycled catalyst was less active in the PhSeH addition to **1a**; the yield of the reaction decreased from 90% to 61% and 41% at the second and third cycles, respectively, after 10 min at 40 °C (entries 1–3, Table 5). SEM study of the recycled catalyst indicated that nanosized building units still are the major form of the catalyst (Figure 3B), although there is a clear tendency of their aggregation to form larger particles (cf. entries 5 and 7, Table 2).

Another approach to catalyst reuse involves addition of fresh portions of the reagents after completing the reaction ("fresh start"). Catalyst activity was also decreased at the second and third cycles under "fresh start" conditions; however the yields were significantly higher compared to the catalyst isolation case (Table 5). This study indicates that catalyst aging takes place during the course of the reaction and during the catalyst isolation from the native media. The latter process is more harmful for the catalyst than the former.

### 3. Conclusions

The present catalytic system is a rare case where heterogeneous reaction conditions provide higher activity and better

selectivity than corresponding homogeneous reactions involving metal complexes with phosphine ligands. It was found that the yield of the addition reaction depends on the catalyst particle size and rapidly increases upon decreasing the particle size into the nanosized region. The findings show that catalyst activity and selectivity can be controlled by adjusting the size and shape of catalyst particles rather than varying metals and ligands.

We have developed a very simple and practical Ni-based catalytic system for the Se–H bond addition to alkynes. High selectivity and yields were achieved under solvent-free conditions at mild temperature. On the basis of the studied catalytic system a new synthetic procedure has been developed for PhSeH addition to the triple bond of terminal and internal alkynes. It is the first example of transition metal-catalyzed Se–H bond addition to internal alkynes. For synthetic purposes it was very useful to replace expensive Pd and Pt catalysts by easily available Ni complexes.<sup>29</sup>

A mechanistic investigation revealed that insoluble [Ni(SePh)<sub>2</sub>]<sub>n</sub> species represent an active form of the catalyst, involving alkyne insertion into the Ni–Se bond as a key step of the catalytic cycle. It is important to note that no additional ligands are required for the developed catalytic systems: one of the reagents (PhSeH) acts as a suitable ligand to maintain proper structure of the catalyst. Investigation of the catalyst with scanning electron microscopy revealed two unusual features of the catalytic system: (1) the formation of support and catalyst in a single chemical stage upon reacting the catalyst precursor with substrate in the case of NiCl<sub>2</sub>/Et<sub>3</sub>N and (2) the formation of a self-organized catalytic system consisting of nanosized building units in the case of Ni(acac)<sub>2</sub>.

## 4. Experimental Section

**4.1. General Procedures.** Unless otherwise noted, the synthetic work was carried out under an argon atmosphere. The alkynes **1f**<sup>30</sup> and **1g**<sup>31</sup> were prepared according to published procedures. Other reagents were obtained from Acros and Lancaster and used as supplied (checked by NMR before use). Ni(acac)<sub>2</sub> was dried in a vacuum (0.01–0.02 Torr, 60 °C, 30 min) before use. Solvents were purified according to published methods.

All NMR measurements were performed using a three-channel Bruker DRX-500 spectrometer operating at 500.1, 125.8, and 95.4 MHz for <sup>1</sup>H, <sup>13</sup>C, and <sup>77</sup>Se nuclei, respectively. The spectra were processed on a Silicon Graphics workstation using the XWINMR software package. All 2D spectra were recorded using an inverse triple resonance probehead with an active shielded Z-gradient coil. <sup>1</sup>H and <sup>13</sup>C chemical shifts are reported relative to the corresponding solvent signals used as internal reference; external Ph<sub>2</sub>Se<sub>2</sub>/CDCl<sub>3</sub> (δ = 463.0 ppm) was used for <sup>77</sup>Se. Estimated errors in the yield determinations by <sup>1</sup>H NMR were <2% (Tables 1, 3–5). 2D <sup>1</sup>H–<sup>77</sup>Se HMQC and NOESY NMR experiments were carried out as described previously.<sup>32</sup>

**4.2. General Synthetic Procedure for **2a–2i**, **9j–9p**, and **10k–10p**.** The alkyne (1.0 × 10<sup>−3</sup> mol) was added to Ni(acac)<sub>2</sub> (2.0 × 10<sup>−5</sup> mol), and the reaction mixture was stirred at room temperature until a uniform green suspension was formed (ca. 5–10 min). PhSeH (1.2 × 10<sup>−3</sup> mol) was added to the stirred mixture at ca. 5 °C (water/ice bath). The stirring was continued for additional

(29) Consider the cost of 1 mmol of Ni(acac)<sub>2</sub>, Pd(acac)<sub>2</sub>, and Pt(acac)<sub>2</sub>: \$2, \$17, and \$102, respectively (Aldrich Catalog, 2006).

(30) Scott, L. T.; DeCicco, G. J.; Hyun, J. L.; Reinhardt, G. *J. Am. Chem. Soc.*, **1985**, *107*, 6546.

(31) Chakraborti, A. K.; Sharma, L.; Gulhane, R.; Shivani. *Tetrahedron* **2003**, *59*, 7661.

(32) Ananikov, V. P.; Beletskaya, I. P. *Russ. Chem. Bull. Int. Ed.* **2003**, *52*, 811.

10 min, and the color of the suspension changed from green to dark. The reaction was carried out at 20–60 °C under stirring until complete conversion of the alkyne.<sup>33</sup> See Tables 3 and 4 for the estimation of reaction time and temperature.

After completion of the reaction the products were purified by flash chromatography on silica with hexane/ethyl acetate gradient elution. After drying in a vacuum the pure products were obtained. The isolated yields given below were calculated on the basis of initial amounts of the alkyne. In all cases the structures of the products were confirmed with <sup>1</sup>H, <sup>13</sup>C, and <sup>77</sup>Se NMR. The stereochemistry was determined using 2D NOESY, LR-COSY, <sup>1</sup>H–<sup>13</sup>C HSQC, <sup>1</sup>H–<sup>13</sup>C HMBC, and <sup>1</sup>H–<sup>77</sup>Se HMQC NMR experiments.

**2-(Phenylseleno)-3-hydroxy-1-butene, H<sub>2</sub>C=C(SePh)-C(OH)(CH<sub>3</sub>)<sub>2</sub> (2a):** colorless oil, 65%. <sup>1</sup>H NMR (500 MHz; CDCl<sub>3</sub>; δ, ppm; *J*, Hz): 1.51 (s, 6H); 2.28 (s, 1H); 4.93 (s, 1H); 5.72 (s, 1H); 7.29–7.33 (m, 3H); 7.57–7.61 (m, 2H). <sup>13</sup>C{<sup>1</sup>H} NMR (126 MHz; CDCl<sub>3</sub>; δ, ppm): 29.69; 74.48; 113.63; 127.90; 129.27; 129.53; 135.00; 153.26. <sup>77</sup>Se NMR (95 MHz, CDCl<sub>3</sub>; δ, ppm): 381.6. Anal. Calcd for C<sub>11</sub>H<sub>14</sub>OSe: C 54.78; H 5.85; Se 32.74. Found: C 54.68; H 5.84; Se 33.10. MS (EI): *m/e* 242 (M<sup>+</sup> 20%).

**2-(Phenylseleno)hexene, H<sub>2</sub>C=C(SePh)CH<sub>2</sub>CH<sub>2</sub>CH<sub>2</sub>CH<sub>3</sub> (2b):** yellow oil, 62%. The product was identified according to the published data.<sup>14</sup>

**2-(Phenylseleno)-4-hydroxy-1-butene, H<sub>2</sub>C=C(SePh)-CH<sub>2</sub>CH<sub>2</sub>OH (2c):** yellow oil, 72%. <sup>1</sup>H NMR (500 MHz; CDCl<sub>3</sub>; δ, ppm; *J*, Hz): 2.06 (br s, 1H); 2.51 (t, 2H, *J* = 5.50); 3.74 (t, 2H, *J* = 5.50); 5.25 (s, 1H); 5.59 (s, 1H); 7.28–7.32 (m, 3H); 7.52–7.57 (m, 2H). <sup>13</sup>C{<sup>1</sup>H} NMR (126 MHz; CDCl<sub>3</sub>; δ, ppm): 41.12; 60.85; 119.06; 127.89; 128.99; 129.24; 134.53; 139.12. <sup>77</sup>Se NMR (95 MHz, CDCl<sub>3</sub>; δ, ppm): 420.2. Anal. Calcd for C<sub>10</sub>H<sub>12</sub>OSe: C 52.87; H 5.32; Se 34.76. Found: C 53.07; H 5.45; Se 34.58. MS (EI): *m/e* 228 (M<sup>+</sup> 15%).

**2-(Phenylseleno)-3-methyl-1-butene, H<sub>2</sub>C=C(SePh)C(CH<sub>3</sub>)<sub>3</sub> (2d):** light yellow oil, 71%. <sup>1</sup>H NMR (500 MHz; CDCl<sub>3</sub>; δ, ppm; *J*, Hz): 1.23 (s, 9H); 4.91 (s, 1H); 5.60 (s, 1H); 7.26–7.30 (m, 3H); 7.54–7.59 (m, 2H). <sup>13</sup>C{<sup>1</sup>H} NMR (126 MHz; CDCl<sub>3</sub>; δ, ppm): 29.93; 38.97; 113.97; 127.53; 129.18; 130.57; 134.79; 155.43. <sup>77</sup>Se NMR (95 MHz, CDCl<sub>3</sub>; δ, ppm): 385.9. Anal. Calcd for C<sub>12</sub>H<sub>16</sub>Se: C 60.25; H 6.74; Se 33.01. Found: C 60.29; H 6.83; Se 33.25. MS (EI): *m/e* 240 (M<sup>+</sup> 17%).

**2-(Phenylseleno)-3-hydroxy-3-methyl-1-pentene, H<sub>2</sub>C=C(SePh)C(OH)(CH<sub>3</sub>)CH<sub>2</sub>CH<sub>3</sub> (2e):** light yellow oil, 74%. <sup>1</sup>H NMR (500 MHz; CDCl<sub>3</sub>; δ, ppm; *J*, Hz): 0.92 (t, 3H, *J* = 7.33); 1.46 (s, 3H); 1.80 (q, 2H, *J* = 7.33); 2.26 (s, 1H); 4.94 (s, 1H); 5.66 (s, 1H); 7.30–7.34 (m, 3H); 7.59–7.63 (m, 2H). <sup>13</sup>C{<sup>1</sup>H} NMR (126 MHz; CDCl<sub>3</sub>; δ, ppm): 8.24; 27.25; 34.16; 77.00; 113.65; 128.00; 129.25; 129.38; 135.44; 151.93. <sup>77</sup>Se NMR (95 MHz, CDCl<sub>3</sub>; δ, ppm): 389.1. Anal. Calcd for C<sub>12</sub>H<sub>16</sub>OSe: C 56.47; H 6.32; Se 30.94. Found: C 56.70; H 6.43; Se 30.67. MS (EI): *m/e* 256 (M<sup>+</sup> 11%).

**1-(Phenylseleno)-1-(1-methoxycyclohexyl)ethene, H<sub>2</sub>C=C(SePh)C<sub>6</sub>H<sub>11</sub>(OCH<sub>3</sub>) (2f):** light yellow oil, 88%. <sup>1</sup>H NMR (500 MHz; CDCl<sub>3</sub>; δ, ppm; *J*, Hz): 1.17–1.27 (m, 1H); 1.52–1.68 (m, 7H); 2.03–2.10 (m, 2H); 3.18 (s, 3H); 4.86 (s, 1H); 5.55 (s, 1H); 7.29–7.35 (m, 3H); 7.59–7.62 (m, 2H). <sup>13</sup>C{<sup>1</sup>H} NMR (126 MHz; CDCl<sub>3</sub>; δ, ppm): 21.82; 25.84; 34.40; 49.81; 79.03; 113.37; 128.11; 128.93; 129.25; 136.56; 152.73. <sup>77</sup>Se NMR (95 MHz, CDCl<sub>3</sub>; δ, ppm): 403.8. Anal. Calcd for C<sub>15</sub>H<sub>20</sub>OSe: C 61.01; H 6.83; Se 26.74. Found: C 61.06; H 6.94; Se 27.02. MS (EI): *m/e* 296 (M<sup>+</sup> 3%).

**2-(Phenylseleno)-3-acetoxy-3-methyl-1-butene, H<sub>2</sub>C=C(SePh)C(OOC-CH<sub>3</sub>)(CH<sub>3</sub>)<sub>2</sub> (2g):** light yellow oil, 85%. <sup>1</sup>H NMR (500 MHz; CDCl<sub>3</sub>; δ, ppm; *J*, Hz): 1.68 (s, 6H); 2.02 (s, 3H); 4.88 (s, 1H); 5.64 (s, 1H); 7.28–7.34 (m, 3H); 7.57–7.62 (m, 2H). <sup>13</sup>C{<sup>1</sup>H} NMR (126 MHz; CDCl<sub>3</sub>; δ, ppm): 22.06; 27.32; 82.96;

113.53; 128.20; 128.64; 129.31; 135.77; 149.70; 169.67. <sup>77</sup>Se NMR (95 MHz, CDCl<sub>3</sub>; δ, ppm): 399.5. Anal. Calcd for C<sub>13</sub>H<sub>16</sub>O<sub>2</sub>Se: C 55.13; H 5.69; Se 27.88. Found: C 55.12; H 5.65; Se 28.12. MS (EI): *m/e* 284 (M<sup>+</sup> 7%).

**1-(Phenylseleno)-1-phenylethene, H<sub>2</sub>C=C(SePh)Ph (2h):** yellow oil, 75%. <sup>1</sup>H NMR (500 MHz; CDCl<sub>3</sub>; δ, ppm; *J*, Hz): 5.36 (s, 1H); 5.88 (s, 1H); 7.16–7.31 (m, 6H); 7.48–7.64 (m, 4H). MS (EI): *m/e* 260 (M<sup>+</sup> 4%). Isolated as a mixture of products **2h–4h**.

**E-3-(Phenylseleno)-3-hexene, CH<sub>3</sub>–CH<sub>2</sub>–CH=C(SePh)CH<sub>2</sub>–CH<sub>3</sub> (9j):** light yellow oil, 73%. <sup>1</sup>H NMR (500 MHz; CDCl<sub>3</sub>; δ, ppm; *J*, Hz): 1.00 (t, 3H, *J* = 7.33); 1.02 (t, 3H, *J* = 7.33); 2.13 (m, 2H, *J*<sub>1</sub> = *J*<sub>2</sub> = 7.33); 2.26 (q, 2H, *J* = 7.33); 5.93 (t, 1H, *J* = 7.33); 7.17–7.25 (m, 3H); 7.42–7.47 (m, 2H). <sup>13</sup>C{<sup>1</sup>H} NMR (126 MHz; CDCl<sub>3</sub>; δ, ppm): 13.87; 14.09; 22.60; 26.14; 126.56; 128.91; 130.98; 132.18; 132.93; 139.19. <sup>77</sup>Se NMR (95 MHz, CDCl<sub>3</sub>; δ, ppm): 424.1. Anal. Calcd for C<sub>12</sub>H<sub>16</sub>Se: C 60.25; H 6.74; Se 33.01. Found: C 60.33; H 6.77; Se 32.79. MS (EI): *m/e* 240 (M<sup>+</sup> 18%).

**E-3-(Phenylseleno)-2-hexene, CH<sub>3</sub>–CH=C(SePh)CH<sub>2</sub>CH<sub>2</sub>CH<sub>3</sub> (9k):** light yellow oil, 53%. <sup>1</sup>H NMR (500 MHz; CDCl<sub>3</sub>; δ, ppm; *J*, Hz): 0.86 (t, 3H, *J* = 7.33); 1.52 (m, 2H, *J*<sub>1</sub> = *J*<sub>2</sub> = 7.33); 1.71 (d, 3H, *J* = 6.87); 2.24 (t, 2H, *J* = 7.33); 6.01 (q, 1H, *J* = 6.87); 7.16–7.26 (m, 3H); 7.42–7.47 (m, 2H). <sup>13</sup>C{<sup>1</sup>H} NMR (126 MHz; CDCl<sub>3</sub>; δ, ppm): 13.43; 14.99; 21.79; 34.30; 126.63; 128.89; 130.50; 132.11; 132.43; 137.40. <sup>77</sup>Se NMR (95 MHz, CDCl<sub>3</sub>; δ, ppm): 428.7. Anal. Calcd for C<sub>12</sub>H<sub>16</sub>Se: C 60.25; H 6.74; Se 33.01. Found: C 60.46; H 6.95; Se 33.20. MS (EI): *m/e* 240 (M<sup>+</sup> 18%).

**E-2-(Phenylseleno)-2-hexene, CH<sub>3</sub>–C(SePh)=CHCH<sub>2</sub>CH<sub>2</sub>CH<sub>3</sub> (10k):** light yellow oil, 28%. <sup>1</sup>H NMR (500 MHz; CDCl<sub>3</sub>; δ, ppm; *J*, Hz): 0.91 (t, 3H, *J* = 7.33); 1.42 (m, 2H, *J*<sub>1</sub> = *J*<sub>2</sub> = 7.33); 1.99 (d, 3H, *J* = 1.37); 2.08 (dt, 2H, *J*<sub>1</sub> = *J*<sub>2</sub> = 7.33); 5.95 (m, 1H, *J*<sub>1</sub> = 7.33, *J*<sub>2</sub> = 1.37); 7.16–7.26 (m, 3H); 7.42–7.47 (m, 2H). <sup>13</sup>C{<sup>1</sup>H} NMR (126 MHz; CDCl<sub>3</sub>; δ, ppm): 13.68; 19.94; 22.38; 31.49; 126.70; 128.93; 130.88; 131.90; 132.46; 136.11. <sup>77</sup>Se NMR (95 MHz, CDCl<sub>3</sub>; δ, ppm): 469.0.

**E-3-(Phenylseleno)-4-hydroxy-2-hexene, CH<sub>3</sub>–CH=C(SePh)–CH(OH)CH<sub>2</sub>CH<sub>3</sub> (9l):** light yellow oil, 65%. <sup>1</sup>H NMR (500 MHz; CDCl<sub>3</sub>; δ, ppm; *J*, Hz): 0.88 (t, 3H, *J* = 7.33); 1.51–1.60 (m, 1H); 1.62–1.72 (m, 1H); 1.80 (d, 3H, *J* = 7.33); 2.04 (d, 1H, *J* = 7.33); 4.51 (dt, 1H, *J*<sub>1</sub> = *J*<sub>2</sub> = 7.33); 6.04 (q, 1H, *J* = 7.33); 7.22–7.28 (m, 3H); 7.50–7.54 (m, 2H). <sup>13</sup>C{<sup>1</sup>H} NMR (126 MHz; CDCl<sub>3</sub>; δ, ppm): 9.87; 15.23; 29.85; 71.76; 126.96; 129.06; 131.10; 132.45; 134.71; 136.68. <sup>77</sup>Se NMR (95 MHz, CDCl<sub>3</sub>; δ, ppm): 345.3. Anal. Calcd for C<sub>12</sub>H<sub>16</sub>OSe: C 56.47; H 6.32; Se 30.94. Found: C 56.34; H 6.29; Se 31.02. MS (EI): *m/e* 256 (M<sup>+</sup> 22%).

**E-2-(Phenylseleno)-4-hydroxy-2-hexene, CH<sub>3</sub>–C(SePh)=CH–CH(OH)CH<sub>2</sub>CH<sub>3</sub> (10l):** light yellow oil, 17%. <sup>1</sup>H NMR (500 MHz; CDCl<sub>3</sub>; δ, ppm; *J*, Hz): 0.90 (t, 3H, *J* = 6.87); 1.44–1.53 (m, 1H); 1.57–1.66 (m, 1H); 2.04 (s, 3H); 4.30 (dt, 1H, *J*<sub>1</sub> = 8.71, *J*<sub>2</sub> = 6.87); 5.74 (d, 1H, *J* = 8.71); 7.26–7.31 (m, 3H); 7.48–7.54 (m, 2H). <sup>13</sup>C{<sup>1</sup>H} NMR (126 MHz; CDCl<sub>3</sub>; δ, ppm): 9.59; 20.04; 30.19; 70.33; 127.66; 128.91; 129.17; 130.62; 134.17; 135.80. <sup>77</sup>Se NMR (95 MHz, CDCl<sub>3</sub>; δ, ppm): 470.1. Anal. Calcd for C<sub>12</sub>H<sub>16</sub>OSe: C 56.47; H 6.32; Se 30.94. Found: C 56.44; H 6.41; Se 31.24. MS (EI): *m/e* 256 (M<sup>+</sup> 2%).

**E-3-(Phenylseleno)-3-penten-1-ol, CH<sub>3</sub>–CH=C(SePh)CH<sub>2</sub>–CH<sub>2</sub>OH (9m):** colorless oil, 54%. <sup>1</sup>H NMR (500 MHz; CDCl<sub>3</sub>; δ, ppm; *J*, Hz): 1.65 (br s, 1H); 1.78 (d, 3H, *J* = 6.87); 2.56 (t, 2H, *J* = 6.42); 3.73 (t, 2H, *J* = 6.42); 6.19 (q, 1H, *J* = 6.87); 7.23–7.27 (m, 3H); 7.43–7.48 (m, 2H). <sup>13</sup>C{<sup>1</sup>H} NMR (126 MHz; CDCl<sub>3</sub>; δ, ppm): 15.23; 35.43; 61.26; 127.06; 128.20; 129.13; 130.27; 132.57; 135.05. <sup>77</sup>Se NMR (95 MHz, CDCl<sub>3</sub>; δ, ppm): 430.3. Anal. Calcd for C<sub>11</sub>H<sub>14</sub>OSe: C 54.78; H 5.85; Se 32.74. Found: C 54.80; H 5.72; Se 32.51. MS (EI): *m/e* 242 (M<sup>+</sup> 55%).

**E-4-(Phenylseleno)-3-penten-1-ol, CH<sub>3</sub>–C(SePh)=CHCH<sub>2</sub>–CH<sub>2</sub>OH (10m):** colorless oil, 36%. <sup>1</sup>H NMR (500 MHz; CDCl<sub>3</sub>; δ, ppm; *J*, Hz): 1.79 (br s, 1H); 2.02 (s, 3H); 2.38 (dt, 2H, *J*<sub>1</sub> = 6.42, *J*<sub>2</sub> = 7.33); 3.66 (d, 2H, *J* = 6.42); 5.89 (t, 1H, *J* = 7.33);

(33) NMR monitoring (or GC) is the easiest way to determine appropriate reaction time.

7.24–7.29 (m, 3H); 7.45–7.50 (m, 2H).  $^{13}\text{C}\{^1\text{H}\}$  NMR (126 MHz;  $\text{CDCl}_3$ ;  $\delta$ , ppm): 20.00; 32.95; 61.81; 127.18; 129.09; 129.16; 131.51; 133.19; 137.79.  $^{77}\text{Se}$  NMR (95 MHz,  $\text{CDCl}_3$ ;  $\delta$ , ppm): 470.4. Anal. Calcd for  $\text{C}_{11}\text{H}_{14}\text{OSe}$ : C 54.78; H 5.85; Se 34.74. Found: C 54.60; H 5.76; Se 32.83. MS (EI):  $m/e$  242 ( $\text{M}^+$  30%).

**E-2-(Phenylseleno)-2-buten-1-ol,  $\text{CH}_3\text{—CH}=\text{C}(\text{SePh})\text{CH}_2\text{OH}$  (9n):** colorless oil, 51%.  $^1\text{H}$  NMR (500 MHz;  $\text{CDCl}_3$ ;  $\delta$ , ppm;  $J$ , Hz): 1.83 (d, 3H,  $J = 6.87$ ); 1.96 (t, 1H,  $J = 5.96$ ); 4.21 (d, 2H,  $J = 5.96$ ); 6.22 (q, 1H,  $J = 6.87$ ); 7.23–7.29 (m, 3H); 7.45–7.50 (m, 2H).  $^{13}\text{C}\{^1\text{H}\}$  NMR (126 MHz;  $\text{CDCl}_3$ ;  $\delta$ , ppm): 15.16; 60.45; 127.19; 129.21; 129.83; 131.92; 132.40; 135.74.  $^{77}\text{Se}$  NMR (95 MHz,  $\text{CDCl}_3$ ;  $\delta$ , ppm): 383.3. Anal. Calcd for  $\text{C}_{10}\text{H}_{12}\text{OSe}$ : C 52.87; H 5.32; Se 34.76. Found: C 52.99; H 5.34; Se 34.86. MS (EI):  $m/e$  228 ( $\text{M}^+$  35%).

**E-3-(Phenylseleno)-2-buten-1-ol,  $\text{CH}_3\text{—C}(\text{SePh})=\text{CHCH}_2\text{OH}$  (10n):** light yellow oil, 32%.  $^1\text{H}$  NMR (500 MHz;  $\text{CDCl}_3$ ;  $\delta$ , ppm;  $J$ , Hz): 1.51 (br s, 1H); 2.03 (s, 3H); 4.17 (d, 2H,  $J = 5.50$ ); 5.89 (t, 1H,  $J = 5.50$ ); 7.27–7.33 (m, 3H); 7.50–7.55 (m, 2H).  $^{13}\text{C}\{^1\text{H}\}$  NMR (126 MHz;  $\text{CDCl}_3$ ;  $\delta$ , ppm): 19.60; 59.59; 127.83; 128.70; 129.21; 131.05; 131.85; 134.54.  $^{77}\text{Se}$  NMR (95 MHz,  $\text{CDCl}_3$ ;  $\delta$ , ppm): 467.0. Anal. Calcd for  $\text{C}_{10}\text{H}_{12}\text{OSe}$ : C 52.87; H 5.32; Se 34.76. Found: C 53.01; H 5.40; Se 35.08. MS (EI):  $m/e$  228 ( $\text{M}^+$  29%).

**E-3-(Phenyl)-2-(phenylseleno)-2-propen-1-ol,  $\text{Ph—CH}=\text{C}(\text{SePh})\text{CH}_2\text{OH}$  (9o):** yellow oil, 62%.  $^1\text{H}$  NMR (500 MHz;  $\text{CDCl}_3$ ;  $\delta$ , ppm;  $J$ , Hz): 2.58 (t, 1H,  $J = 5.96$ ); 4.36 (d, 2H,  $J = 5.96$ ); 6.94 (s, 1H); 7.19–7.31 (m, 8H); 7.53–7.57 (m, 2H).  $^{13}\text{C}\{^1\text{H}\}$  NMR (126 MHz;  $\text{CDCl}_3$ ;  $\delta$ , ppm): 61.44; 127.43; 127.69; 128.30; 128.44; 129.04; 129.30; 133.69; 135.84; 136.15.  $^{77}\text{Se}$  NMR (95 MHz,  $\text{CDCl}_3$ ;  $\delta$ , ppm): 409.7. Anal. Calcd for  $\text{C}_{15}\text{H}_{14}\text{OSe}$ : C 62.29; H 4.88; Se 27.30. Found: C 62.27; H 4.89; Se 27.32. MS (EI):  $m/e$  290 ( $\text{M}^+$  24%).

**E-3-(Phenyl)-3-(phenylseleno)-2-propen-1-ol,  $\text{Ph—C}(\text{SePh})=\text{CHCH}_2\text{OH}$  (10o):** yellow oil, 29%.  $^1\text{H}$  NMR (500 MHz;  $\text{CDCl}_3$ ;  $\delta$ , ppm;  $J$ , Hz): 1.90 (br s, 1H); 3.99 (d, 2H,  $J = 6.42$ ); 5.94 (t, 1H,  $J = 6.42$ ); 7.18–7.29 (m, 8H); 7.46–7.50 (m, 2H).  $^{13}\text{C}\{^1\text{H}\}$  NMR (126 MHz;  $\text{CDCl}_3$ ;  $\delta$ , ppm): 60.44; 127.96; 127.99; 128.04; 128.89; 129.14; 130.31; 134.86; 136.87; 137.92.  $^{77}\text{Se}$  NMR (95 MHz,  $\text{CDCl}_3$ ;  $\delta$ , ppm): 481.9. Anal. Calcd for  $\text{C}_{15}\text{H}_{14}\text{OSe}$ : C 62.29; H 4.88; Se 27.30. Found: C 62.36; H 4.92; Se 27.23. MS (EI):  $m/e$  290 ( $\text{M}^+$  18%).

**E-1-(Phenyl)-2-(phenylseleno)-1-butene,  $\text{Ph—CH}=\text{C}(\text{SePh})\text{—CH}_2\text{CH}_3$  (9p):** yellow oil, 72%.  $^1\text{H}$  NMR (500 MHz;  $\text{CDCl}_3$ ;  $\delta$ , ppm;  $J$ , Hz): 1.19 (t, 3H,  $J = 7.33$ ); 2.49 (q, 2H,  $J = 7.33$ ); 6.82 (s, 1H); 7.12–7.17 (m, 2H); 7.18–7.24 (m, 3H); 7.25–7.28 (m, 3H); 7.54–7.59 (m, 2H).  $^{13}\text{C}\{^1\text{H}\}$  NMR (126 MHz;  $\text{CDCl}_3$ ;  $\delta$ , ppm): 14.06; 26.56; 126.81; 127.41; 128.20; 128.29; 129.16; 133.29; 133.76; 137.23; 138.75; 139.36.  $^{77}\text{Se}$  NMR (95 MHz,  $\text{CDCl}_3$ ;  $\delta$ , ppm): 437.3. Anal. Calcd for  $\text{C}_{16}\text{H}_{16}\text{Se}$ : C 66.90; H 5.61; Se 27.49. Found: C 66.76; H 5.65; Se 27.29. MS (EI):  $m/e$  288 ( $\text{M}^+$  31%).

**E-1-(Phenyl)-1-(phenylseleno)-1-butene,  $\text{Ph—C}(\text{SePh})=\text{CHCH}_2\text{—CH}_3$  (10p):** yellow liquid, 21%.  $^1\text{H}$  NMR (500 MHz;  $\text{CDCl}_3$ ;  $\delta$ , ppm;  $J$ , Hz): 0.95 (t, 3H,  $J = 7.33$ ); 2.08 (m, 2H,  $J_1 = J_2 = 7.33$ ); 6.13 (t, 1H,  $J = 7.33$ ); 7.18–7.28 (m, 5H); 7.29–7.33 (m, 3H); 7.39–7.43 (m, 2H).  $^{13}\text{C}\{^1\text{H}\}$  NMR (126 MHz;  $\text{CDCl}_3$ ;  $\delta$ , ppm): 14.15; 24.09; 126.99; 127.19; 127.81; 128.83; 129.10; 129.81; 130.44; 130.52; 131.41; 133.07.  $^{77}\text{Se}$  NMR (95 MHz,  $\text{CDCl}_3$ ;  $\delta$ , ppm): 487.3. Anal. Calcd for  $\text{C}_{16}\text{H}_{16}\text{Se}$ : C 66.90; H 5.61; Se 27.49. Found: C 66.76; H 5.65; Se 27.29. MS (EI):  $m/e$  288 ( $\text{M}^+$  31%).

**4.3. Preparation of  $[\text{M}(\text{SePh})_2]_n$  from Different Precursors ( $\text{M} = \text{Pd}, \text{Ni}$ ). A.  $\text{Pd}(\text{OAc})_2$ ,  $\text{NiCl}_2$ ,  $\text{Ni}(\text{OAc})_2$ , and  $\text{Ni}(\text{acac})_2$  Precursors.** The alkyne **1a** (0.084 g,  $1.0 \times 10^{-3}$  mol) was added to the metal compound ( $5.0 \times 10^{-5}$  mol) and stirred until a homogeneous dark brown suspension was formed (ca. 5–10 min). PhSeH (0.189 g,  $1.2 \times 10^{-3}$  mol) was added to the stirred

suspension at ca. 5 °C (water/ice bath), and stirring was continued at 25 °C for an additional 10 min. A dark brown suspension was formed. The precipitate was separated, washed with ether ( $4 \times 5$  mL), and dried in a vacuum.

**Elemental Analysis.  $[\text{Ni}(\text{SePh})_2]_n$  Made from  $\text{Ni}(\text{acac})_2$  Precursor.** Anal. Calcd for  $\text{C}_{12}\text{H}_{10}\text{NiSe}_2$ : C 38.87; H 2.72; Ni 15.83; Se 42.59. Found: C 38.63; H 2.93; Ni 15.59; Se 42.81.

**$[\text{Ni}(\text{SePh})_2]_n$  Made from  $\text{Ni}(\text{OAc})_2$  Precursor.** Anal. Calcd for  $\text{C}_{12}\text{H}_{10}\text{NiSe}_2$ : C 38.87; H 2.72; Ni 15.83; Se 42.59. Found: C 38.88; H 2.84; Ni 15.73; Se 42.41.

**$[\text{Ni}(\text{SePh})_2]_n/\text{NiCl}_2$  Made from  $\text{NiCl}_2$  Precursor.** Anal. Calcd for  $\text{Ni}(\text{SePh})_2:\text{NiCl}_2 = 1:9$ : C 9.38; H 0.66; Cl 41.51; Ni 38.18; Se 10.27. Found: C 9.33; H 0.44; Cl 41.10; Ni 38.40; Se 10.58.

**SEM Study.**  $\text{Pd}(\text{OAc})_2$  precursor: Figure 1A and entry 1 of Table 2;  $\text{NiCl}_2$  precursor: Figure 1B and entry 2 of Table 2;  $\text{Ni}(\text{OAc})_2$  precursor: Figure 1C and entry 3 of Table 2;  $\text{Ni}(\text{acac})_2$  precursor: Figures 1D and 1E and entry 5 of Table 2.

**B.  $\text{NiCl}_2/\text{Et}_3\text{N}$  System.** The alkyne **1a** (0.084 g,  $1.0 \times 10^{-3}$  mol) and  $\text{Et}_3\text{N}$  (0.010 g,  $1.0 \times 10^{-4}$  mol) were added to  $\text{NiCl}_2 \cdot 6\text{H}_2\text{O}$  (0.011 g,  $5.0 \times 10^{-5}$  mol) and stirred until a uniform suspension was formed (ca. 5–10 min). PhSeH (0.189 g,  $1.2 \times 10^{-3}$  mol) was added to the stirred suspension at ca. 5 °C (water/ice bath), and stirring was continued at 25 °C for an additional 10 min. The color of the suspension changed from green to dark and an insoluble brown-lilac precipitate was formed. The precipitate was separated, washed with ether ( $5 \times 5$  mL), and dried in a vacuum.

**Elemental analysis:** 89% (0.133 g) of a dark brown solid. Anal. Calcd for  $\text{C}_{24}\text{H}_{42}\text{NiSe}_2\text{N}_2\text{Cl}_2$ : C 44.61; H 6.55; Ni 9.08; Se 24.44; Cl 10.97. Found: C 44.25; H 6.33; Ni 9.03; Se 24.11. SEM study: Figures 2A, 2C, 2D and entry 4 of Table 2.

**C. Removing the  $[\text{Et}_3\text{NH}]^+\text{Cl}^-$  Support.** The same as above (4.3B), except that after separation the precipitate was washed with ether ( $6 \times 5$  mL), water ( $3 \times 5$  mL), and acetone ( $4 \times 5$  mL) and dried in a vacuum. SEM study: Figure 2B.

**4.4. Different Order of Reagent Addition. A. Normal Order of Reagent Addition.** The alkyne **1a** ( $1.0 \times 10^{-3}$  mol) was added to  $\text{Ni}(\text{acac})_2$  ( $2.0 \times 10^{-5}$  mol), and the reaction mixture was stirred at 25 °C until a uniform green suspension was formed (ca. 5–10 min). PhSeH ( $1.2 \times 10^{-3}$  mol) was added to the stirred mixture at ca. 5 °C (water/ice bath). The stirring was continued for additional 10 min at 25 °C, the color of the suspension changed from green to dark, and an insoluble crimson precipitate was formed. After that a small aliquot was taken from the mixture and investigated by  $^1\text{H}$  NMR. Product **2a** was formed with 74% yield (determined by  $^1\text{H}$  NMR).

**B. Reversed Order of Reagent Addition.** PhSeH ( $1.2 \times 10^{-3}$  mol) was added to  $\text{Ni}(\text{acac})_2$  ( $2.0 \times 10^{-5}$  mol), and the reaction mixture was stirred at 25 °C until a uniform dark crimson suspension was formed (ca. 5–10 min). Alkyne **1a** ( $1.0 \times 10^{-3}$  mol) was added to the stirred mixture at ca. 5 °C (water/ice bath). The stirring was continued for additional 10 min at 25 °C. After that a small aliquot was taken from the mixture and investigated by  $^1\text{H}$  NMR. Product **2a** was formed with 45% yield (determined by  $^1\text{H}$  NMR). The precipitate was separated, washed with ether ( $4 \times 5$  mL), and dried in a vacuum. SEM study: Figure 3A and entry 6 of Table 2.

**4.5. Reaction of  $[\text{Ni}(\text{SePh})_2]_n$  with Alkyne (Scheme 5).** The alkyne **1a** ( $2.2 \times 10^{-4}$  mol), PhSeH ( $2.2 \times 10^{-4}$  mol), and  $\text{C}_6\text{D}_6$  (0.5 mL) were added to  $[\text{Ni}(\text{SePh})_2]_n$  ( $1.1 \times 10^{-4}$  mol), and the reaction mixture was stirred at 40 °C until complete conversion of the alkyne (ca. 60 min) as confirmed by NMR.

**4.6. Study of catalyst recycling. A. Catalyst Isolation.** The alkyne **1a** ( $1.0 \times 10^{-3}$  mol) was added to  $\text{Ni}(\text{acac})_2$  ( $2.0 \times 10^{-5}$  mol), and the reaction mixture was stirred at 25 °C until a uniform green suspension was formed (ca. 5–10 min). PhSeH ( $1.2 \times 10^{-3}$  mol) was added to stirred mixture at ca. 5 °C (water/ice bath). The



stirring was continued for additional 10 min at 40 °C, the color of the suspension changed from green to dark, and an insoluble crimson precipitate was formed. Small aliquots were taken from the mixture and investigated by  $^1\text{H}$  NMR (see Table 5 for yields). The precipitate was separated, washed with ether ( $4 \times 5$  mL), dried in air, and used in further reactions with the same amounts of **1a** and PhSeH at 40 °C for 10 min. After completing the last cycle the precipitate was separated, washed with ether ( $4 \times 5$  mL), dried in a vacuum, and used for the SEM study (see Figure 3B and entry 7 of Table 2).

**B. "Fresh Start" Procedure.** The first cycle was carried out as described above. After 10 min new portions of **1a** and PhSeH were

added to the reaction mixture. Small aliquots were taken from the mixture and investigated by  $^1\text{H}$  NMR (see Table 5 for yields).

**Acknowledgment.** The work was supported by the Russian Foundation for Basic Research (Project Nos. 04-03-32501 and 05-03-34888) and the Division of Chemistry and Material Sciences of the Russian Academy of Sciences (under program "Theoretical and Experimental Investigation of the Nature of Chemical Bond and Mechanisms of the Most Important Chemical Reactions and Processes").

OM061033B